JOURNAL OF CATALYSIS 123, 43–59 (1990)

Characterization of Silica-Supported Ru–Ag and Ru–Au Bimetallic Catalysts by Hydrogen Chemisorption and NMR of Adsorbed Hydrogen

X. WU,* B. C. GERSTEIN,† AND T. S. KING*,[1]

*Departments of *Chemical Engineering, and †Chemistry, Iowa State University, and Ames Laboratory, Institute for Physical Research and Technology, Ames, Iowa 50011*

Received June 8, 1989; revised November 29, 1989

Silica-supported Ru–Ag and Ru–Au bimetallic catalysts were studied by hydrogen chemisorption and by nuclear magnetic resonance (NMR) of adsorbed hydrogen. Both techniques yielded nearly the same capacity for hydrogen chemisorption on both series of bimetallic catalysts. A small difference measured by the two techniques was attributed to hydrogen spillover from ruthenium onto the silica support. This effect of hydrogen spillover was less pronounced in Ru–Ag/SiO_2 than in Ru–Au/SiO_2, as indicated by the longer spin-lattice relaxation times of the silanol proton. The results of these studies are used to infer that a stronger interaction exists between silver and ruthenium than between gold and ruthenium in the supported bimetallics. Both NMR results and volumetric chemisorption results show that residual chlorine inhibits the hydrogen chemisorption capacity of the Ru/SiO_2 catalyst and Ru–Au/SiO_2 bimetallic catalysts. The variation of the adsorbed hydrogen chemical shift with chlorine coverage indicates an electronic interaction that is due to chlorine adsorption. A direct comparison between clean Ru–Cu/SiO_2 (from a previous study), Ru–Ag/SiO_2, and Ru–Au/SiO_2 bimetallic catalysts was made to illustrate the varying degrees of interaction between ruthenium and copper, silver, or gold.

INTRODUCTION

Among Ru–Group Ib bimetallic catalysts there have been relatively few studies of supported Ru–Ag (*1–3*) and Ru–Au (*4–9*) catalysts, while the Ru–Cu system has been extensively investigated. The lack of interest in the Ru–Ag and Ru–Au bimetallic systems is attributable to the absence of unusual chemisorptive and catalytic behaviors in comparison with the Ru–Cu bimetallic system when silica is used as the support. Except for the Ru–Au/MgO (*6*) bimetallic catalysts, the trends of catalytic activities of Ru–Ag/SiO_2 (*2*) and Ru–Au/SiO_2 (*6*) bimetallic catalysts nearly match those of hydrogen chemisorption measurements.

As in the Ru–Cu alloy, large miscibility gaps exist in both the Ru–Ag and the Ru–Au binary alloys (*10*). However, these two bimetallic systems may behave differently in a highly dispersed state. Previous investigations seem to indicate that when supported on silica, Ru–Ag and Ru–Au do form bimetallic particles for high contents of silver or gold, respectively (*2, 7*). Monte Carlo simulations on silica-supported Ru–Group IB bimetallic particles, (*11, 12*) have indicated that Ag and Au are more strongly segregated at Ru surfaces than Cu, and they tend to form Ag and Au islands at high Ag and Au concentrations.

It is well known that Ag and Au do not dissociatively adsorb molecular hydrogen; they adsorb only atomized hydrogen at temperatures below about 195 K (*13*). Therefore, unlike the Ru–Cu/SiO_2 catalysts where hydrogen can spill over from Ru to Cu (*14, 15*), selective hydrogen chemisorption can be applied directly at room temperature to titrate the amount of Ru exposed at

[1] To whom correspondence should be addressed.

0021-9517/90 $3.00

the surface of the bimetallic particles in $Ru-Ag/SiO_2$ and $Ru-Au/SiO_2$ catalysts. The absence of this metal-to-metal hydrogen spillover simplifies characterization of these supported bimetallic catalysts.

The readily available metal salt $RuCl_3 \cdot nH_2O$ has been used most frequently as a precursor in preparation of supported Ru catalysts and ruthenium-containing bimetallic catalysts except for the Ru–Ag system, where $Ru(NO)(NO_3)_3$ has been used to avoid AgCl precipitation. A number of recent studies (*16–19*) have indicated that chlorine contamination exists on the surfaces of Ru particles in Ru/SiO_2 catalysts prepared from the chloride salt. This chlorine effect not only inhibits adsorption of hydrogen but also influences the catalytic activity of Ru/SiO_2 catalysts. It is likely that $Ru-Au/SiO_2$ catalysts used in the previous investigations were also contaminated by chlorine.

The objective of the present study was to determine the fractions of ruthenium exposed at the surfaces of Ru–Ag and Ru–Au bimetallic particles on clean $Ru-Ag/SiO_2$ and $Ru-Au/SiO_2$ bimetallic catalysts by means of hydrogen chemisorption and nuclear magnetic resonance (NMR) of absorbed hydrogen. These results are compared with those on $Ru-Cu/SiO_2$ bimetallic catalysts from a previous study (*15*). The effect of chlorine on the Ru–Au bimetallic catalysts was also examined in the present study.

EXPERIMENTAL

Catalyst Preparation

The $Ru-Ag/SiO_2$ catalysts were prepared by incipient wetness co-impregnation of a solution of $Ru(NO)(NO_3)_3$ (AESAR) and $AgNO_3$ (AESAR, 99.999%) with a dried Cab-O-Sil HS5 (300 m^2/g BET surface area) silica support. The $Ru-Au/SiO_2$ catalysts were prepared by co-impregnation of a solution of $RuCl_3 \cdot 3H_2O$ (AESAR) and $HAuCl_4 \cdot H_2O$ (AESAR, 99.999%) with the same support. Two Ru/SiO_2 catalysts were prepared from $Ru(NO)(NO_3)_3$ and $RuCl_3 \cdot 3H_2O$, respectively, with the same preparation method. About 2.2 ml of impregnating solution per gram of SiO_2 was used to achieve incipient wetness. The slurries obtained after impregnation were dried for 24 h at room temperature and 4 h in air at 383 K. The ruthenium loading for all catalysts was kept at 4% by total weight of the support and metals. A total of five different $Ru-Ag/SiO_2$ and five different $Ru-Au/SiO_2$ catalysts were prepared to give a wide range of silver and gold loading, respectively.

Volumetric Adsorption Apparatus

The volumetric adsorption apparatus has been described previously (*15, 20*). It consists of a multiport Pyrex glass manifold (127.3 cm^3) in connection with a high-vacuum system, which includes a turbo-molecular pump (Balzers Model TPH050), a forepump trap, and a mechanical pump. The apparatus is capable of flow-through reduction of catalyst samples. High-vacuum greaseless, bakeable stopcocks with Teflon plugs (Ace Glass) and FETFE O-ring seals were used on the manifold to manipulate either storage or dosage of gas, or both, and eliminate hydrocarbon contamination. Pressures inside the manifold were monitored over a wide range from 10^{-7} Torr to 10^3 Torr by a cold cathode vacuum gauge (Varian Model 860A) and two absolute Baratron pressure gauges (MKS).

A flow-through Pyrex cell mounted with a coarse glass frit (35 μm in average pore diameter) was used to contain catalyst samples for the volumetric adsorption experiments. A small matching furnace was used to provide uniform heating around the cell. The temperature inside the furnace was controlled by a proportional temperature controller (Omega) to within ± 1 K.

Catalyst Reduction and Volumetric Adsorption

For the Ru/SiO_2 catalyst prepared from $Ru(NO)(NO_3)_3$ and the $Ru-Ag/SiO_2$ catalysts, reduction by hydrogen was carried

out directly inside the Pyrex cell of the adsorption apparatus. Approximately 1 g of a catalyst sample was loaded into the flow-through cell, which was then attached to one of the sample ports of the manifold. While helium gas was allowed to flow through the sample bed in the cell, the temperature of the cell was raised to 423 K. Then helium was switched off and replaced by hydrogen at a flow rate of 50 cm^3/min. A pre-reduction period of 1 h proceeded at that temperature. The temperature was then raised at 10 K/min to 723 K. Further reduction was carried out for 2 additional hours at 723 K. Helium (99.999%) and hydrogen (99.8%) gases (Liquid Air Co.) were used as received. The sample was then evacuated for 2 h at 723 K to an ultimate pressure of 10^{-6} Torr to remove traces of water and surface hydrogen.

Hydrogen for volumetric adsorption was purified by passing it through a catalytic hydrogen purifier (Engelhard Deoxo) in series with a gas purifier with Drierite and 5-Å molecular sieve (Alltech) to remove traces of oxygen and moisture. Hydrogen adsorption experiments were performed at room temperature (294 K). The total hydrogen adsorption isotherm was measured in the pressure range of 0–30 Torr. The reversible hydrogen adsorption isotherm was collected under the same conditions after a 10-min evacuation period to 10^{-6} Torr following the total adsorption. The irreversible hydrogen uptake was obtained by taking the difference between the values of the total and the reversible isotherms extrapolated to zero pressure. An equilibration time of 4 h was used for the initial dose and 1 h for subsequent doses.

For the Ru/SiO_2 catalyst prepared from $RuCl_3 \cdot 3H_2O$ and the $Ru–Au/SiO_2$ catalysts, two different sample treatment procedures were carried out. First, the catalyst samples were reduced for 4 h and adsorption isotherms measured following the same procedure as described above. Second, the reduced catalyst samples were washed repeatedly in hot distilled water (90–95°C) to eliminate residual chlorine in the catalysts. Successive cycles of wash (one wash consisted of about 20 ml of water per gram sample) and reduction were used for each sample. The washed samples were dried and reduced again in the flow-through cell at 673 K for 2 h followed by a 2-h evacuation period before hydrogen chemisorption measurements were taken. The procedure for hydrogen chemisorption was identical with that for the Ru/SiO_2 catalyst made via a chlorine-free precursor and $Ru–Ag/SiO_2$ catalysts and was carried out on the washed samples after every wash. The water after wash was analyzed by atomic absorption spectroscopy for Ru and Au contents.

NMR Sample Treatment

A needle-bellows assembly made of stainless steel was used for direct reduction of a catalyst sample in flowing hydrogen inside a 5-mm NMR tube (*15*). The syringe needle (18 gauge) was capable of moving vertically by more than 6 cm through adjustable compression and extension of the bellows. Vacuum-tight connections were made between the NMR tube and the needle-bellows assembly and also between the assembly and the manifold described above. In addition, a small cylindrical furnace provided uniform heating around the NMR tube and the temperature of the furnace was controlled to better than ± 1 K.

With helium gas flowing through the needle, the needle was lowered to the bottom of the NMR tube, which contained approximately 60 mg of catalyst sample. The reduction procedure was the same as that previously described for the volumetric adsorption experiment, with a hydrogen flow rate of 15 cm^3/min. After reduction, the needle was lifted out of the sample, and evacuation proceeded for 2 h at the reduction temperature before the sample was allowed to cool to ambient temperature. Up to four samples could be reduced simultaneously. Purified hydrogen was then dosed through the needle separately to each sam-

ple and the system was allowed to equilibrate for 4 h. The NMR tube containing the sample was then immersed in a water bath and sealed off with a micro-torch. The exact sample weight was measured after the NMR tube was sealed by subtracting the tare weight of the tube, which was measured prior to loading the sample.

NMR Experiments

The home-built NMR spectrometer (*21*) used for the present study was operated at 220 MHz for proton resonance. A proton-free probe with a doubly wound coil (*22*) was used for all the NMR measurements. The probe quality factor Q was set at about 100 to obtain the optimal values of sensitivity and ring down time for a fixed pulse power (*23*). A detailed description of the spectrometer's rapid-recovery receiving system has been published elsewhere (*14*).

All NMR spectra were collected under a repetitive 90° single-pulse sequence. The recycle time between rf pulses was set at 0.2 s to selectively suppress the intense signal associated with protons in the silanol group in catalyst samples, which has a relatively long spin-lattice relaxation time T_1 (on the order of seconds). The above repetition rate avoids T_1 saturation of the peak corresponding to hydrogen adsorbed on ruthenium. The total number of scans for data acquisition on each sample was 10,000. The inversion recovery pulse sequence (180°–τ–90°) was applied to measure the spin-lattice relaxation times of the silanol protons (in the time domain) and of the hydrogen adsorbed on ruthenium (in the frequency domain). A pure water sample was used as the reference standard for the observed lineshifts.

For accuracy in spin counting, the water sample was doped with sufficient $FeCl_3$ such that the linewidths of the standard and unknown were comparable. The doped water was sealed in a capillary tube having the same length as the catalyst sample in the NMR tube to offset errors due to B_1 inhomogeneity of the coil. All NMR measurements were taken at ambient temperature (294 ± 1 K).

RESULTS

A set of NMR spectra measured on a 4% Ru/SiO_2 catalyst (prepared from $Ru(NO)(NO_3)_3$) and 4% $Ru–Ag/SiO_2$ catalysts having various silver loadings is shown in Fig. 1. All catalyst samples were under 5 Torr hydrogen gas. As can be seen, two distinct resonance lines were observed: (1) the downfield peak at 4 ± 1 ppm corresponding to the silanol proton from the silica support, and (2) the upfield peak in the range of 64 to 69 ppm corresponding to hydrogen adsorbed on ruthenium surfaces. As the silver content was increased from 0 to 50 at.%, a significant decrease in the upfield peak intensity was observed. Also, there is a moderate increase in linewidth for the upfield peak from 6.3 to 11.2 kHz over the range of silver content mentioned above. An asymmetric feature on the upfield peak for both the Ru/SiO_2 catalyst and the $Ru–Ag/SiO_2$ catalyst with 13.4 at.% Ag can be seen in this figure. In the case of pure Ru/SiO_2 catalyst, this asymmetric feature becomes obvious when compared with a Lorentzian line as shown in the same figure. This asymmetry appeared to have vanished for $Ru–Ag/SiO_2$ catalysts with a silver content of 20 at.% or higher. For these catalysts with higher silver content, the upfield peak was well fitted by a Lorentzian lineshape, as illustrated by the catalyst with 30 at.% Ag in the same figure. In addition, the lineshift for the upfield peak as calculated by the first moment is farther upfield by about 5 ppm for the two $Ru–Ag/SiO_2$ bimetallic catalysts with 20 at.% Ag and 30 at.% Ag than that for the pure Ru/SiO_2 catalyst.

Figure 2 shows four different NMR spectra for Ru/SiO_2 and $Ru–Au/SiO_2$ catalysts prepared by the two different sample treatment methods noted earlier. Note that all catalyst samples were under 5 Torr hydrogen gas. Spectra A and B represent NMR resonances on a 4% Ru/SiO_2 catalyst and a

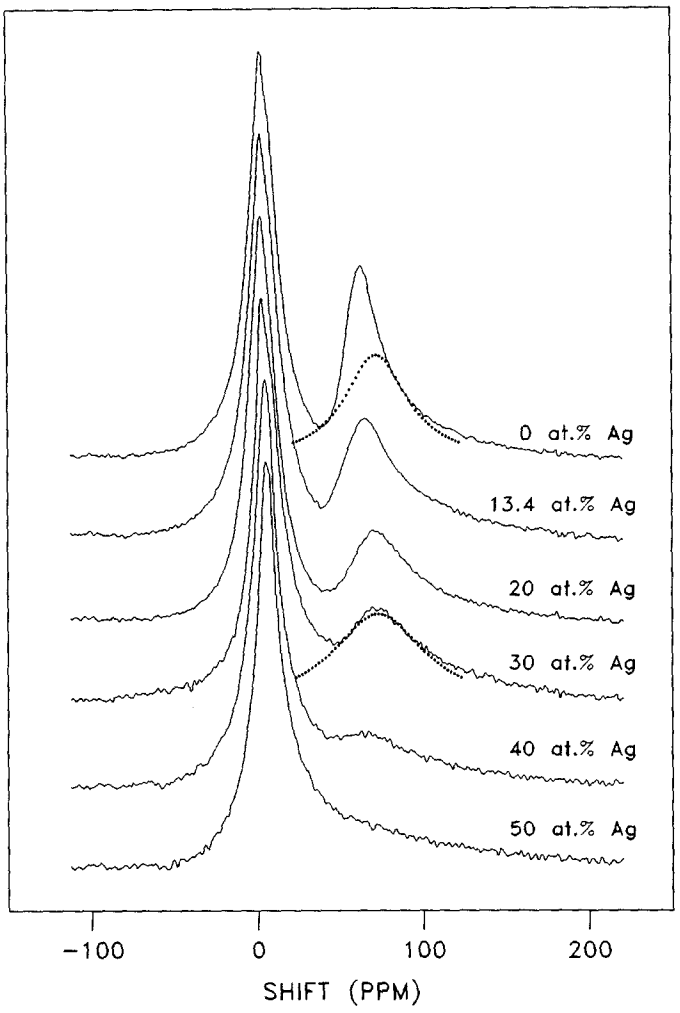

FIG. 1. NMR spectra of adsorbed hydrogen on a series of Ru–Ag/SiO_2 bimetallic catalysts under 5 Torr hydrogen. The silver bulk compositions expressed in atomic percentages are as indicated. A dotted Lorentzian line is drawn under the upfield peak for the catalyst with 0 at.% Ag to show the asymmetry of this peak. Also, the symmetry of the upfield peak for the catalyst with 30 at.% Ag is illustrated by comparison with a dotted Lorentzian line drawn underneath this peak. Water is used as reference for the lineshift.

4% Ru–Au/SiO_2 catalyst with 20 at.% gold content, respectively. These two catalysts were prepared by using $RuCl_3 \cdot 3H_2O$ as a precursor. The sample treatment procedure of repetitive hot water wash as described above was used to eliminate all residual chlorine from these two catalysts. Both spectra showed two well-resolved resonances with a similar lineshape, lineshift, and intensity for the upfield and the downfield peak, respectively. The upfield peaks were asymmetric, as were the peaks for Ru–Ag/SiO_2 catalysts with 0 and 13.4 at.% silver content (Fig. 1). The lineshifts for the upfield peak in both spectrum A and spectrum B were nearly identical at about 67 ppm. And unlike Ru–Ag/SiO_2 catalysts, an increase in the gold content did not result in a significant decrease in the upfield peak intensity for Ru–Au/SiO_2 catalysts. Al-

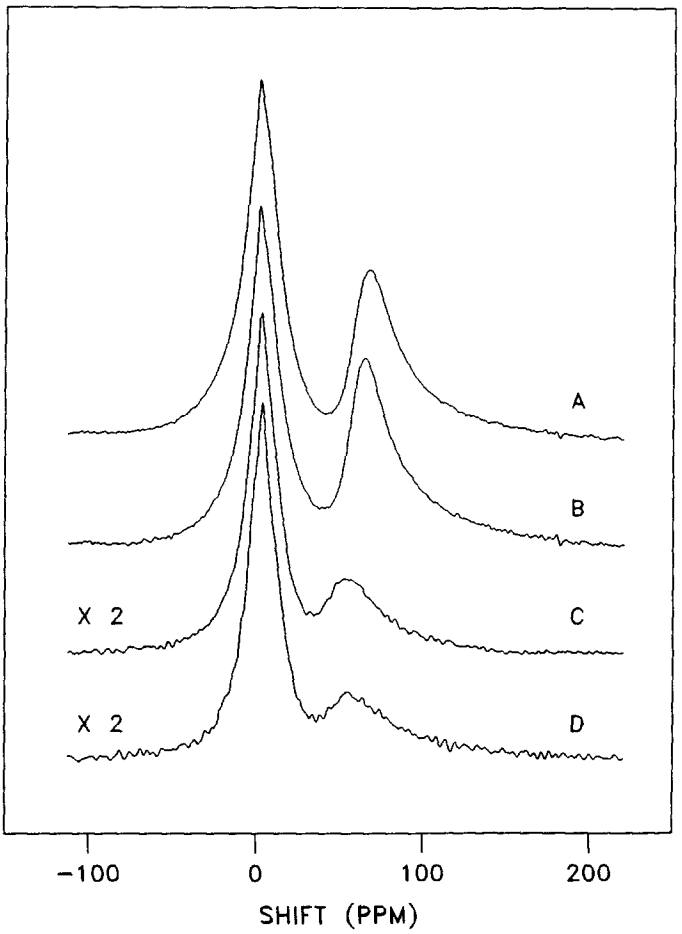

FIG. 2. NMR spectra of adsorbed hydrogen on (A) 4% Ru/SiO_2 (five washes); (B) 4% $Ru–Au/SiO_2$ with 20 at.% Au (five washes); (C) 4% Ru/SiO_2 (not washed); (D) 4% $Ru–Au/SiO_2$ with 20 at.% Au (not washed). All catalyst samples were under 5 Torr hydrogen. Water is used as reference for the lineshift.

though not shown in the figure, the NMR spectrum for a $Ru–Au/SiO_2$ catalyst with 50 at.% gold content (treated with hot water wash) exhibits a spectral feature similar to that of spectrum A or spectrum B.

Also shown in Fig. 2 are spectrum C and spectrum D representing NMR resonances on the same 4% Ru/SiO_2 catalyst and the 4% $Ru–Au/SiO_2$ catalyst with 20 at.% gold content, respectively. However, these two catalysts were treated only by direct hydrogen reduction and were not washed with hot water; thus, they contained a considerable amount of residual chlorine. Clearly, the upfield peak intensities of these two spectra were greatly reduced compared to those of spectrum A and spectrum B (by a factor of about 5). More interestingly, the upfield peaks appear farther downfield at about 52 ppm compared to 67 ppm for the peaks in spectrum A and spectrum B. Similar spectral features were also observed for unwashed $Ru–Au/SiO_2$ catalysts with higher gold contents.

The effectiveness of the hot water washing procedure in eliminating residual chlorine from a Ru/SiO_2 catalysts prepared from $RuCl_3 \cdot 3H_2O$ was first reported by Miura *et al.* (19). This procedure effectively eliminates chlorine from the reduced

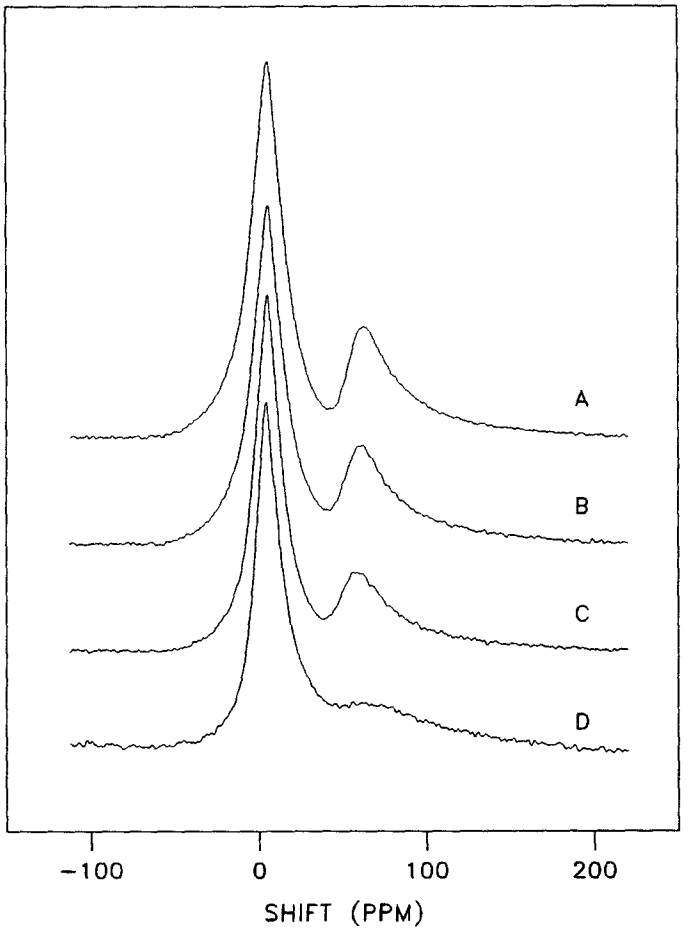

FIG. 3. NMR spectra of the irreversibly adsorbed hydrogen on (A) 4% Ru/SiO_2 (five washes); (B) 4% $Ru–Au/SiO_2$ with 20 at.% Au (five washes); (C) 4% Ru/SiO_2 (prepared from nitrate salt); (D) 4% $Ru–Ag/SiO_2$ with 20 at.% Ag. All catalyst samples were evacuated to 10^{-6} Torr for 10 min after exposure to 5 Torr hydrogen. Water is used as reference for the lineshift.

Ru/SiO_2 catalyst without loss of ruthenium. This finding was verified in the present study by atomic absorption spectroscopy of the water after wash showing only trace amounts of ruthenium (<0.5 ppm). Also, no gold was detected in the water from washing $Ru–Au/SiO_2$ catalysts by this technique, indicating no loss of gold from these catalysts due to the washing procedure.

Figure 3 shows NMR spectra for four different catalysts that were evacuated to 10^{-6} Torr for 10 min after adsorption under 5 Torr hydrogen. Spectrum A and spectrum B represent NMR resonances on a 4% Ru/SiO_2 catalyst and a 4% $Ru–Au/SiO_2$ catalyst with 20 at.% gold content, respectively. Both catalysts were prepared using the chloride metal salts and the reduced catalysts were washed repeatedly with hot water. As shown, these two spectra display nearly identical resonance features in terms of lineshift, lineshape, and intensity. The upfield peaks of these two spectra are more asymmetric and shift slightly farther downfield than those of the corresponding spectra A and B in Fig. 2. Spectrum C and spectrum D in Fig. 3 represent NMR resonances on a 4% Ru/SiO_2 catalyst (prepared from

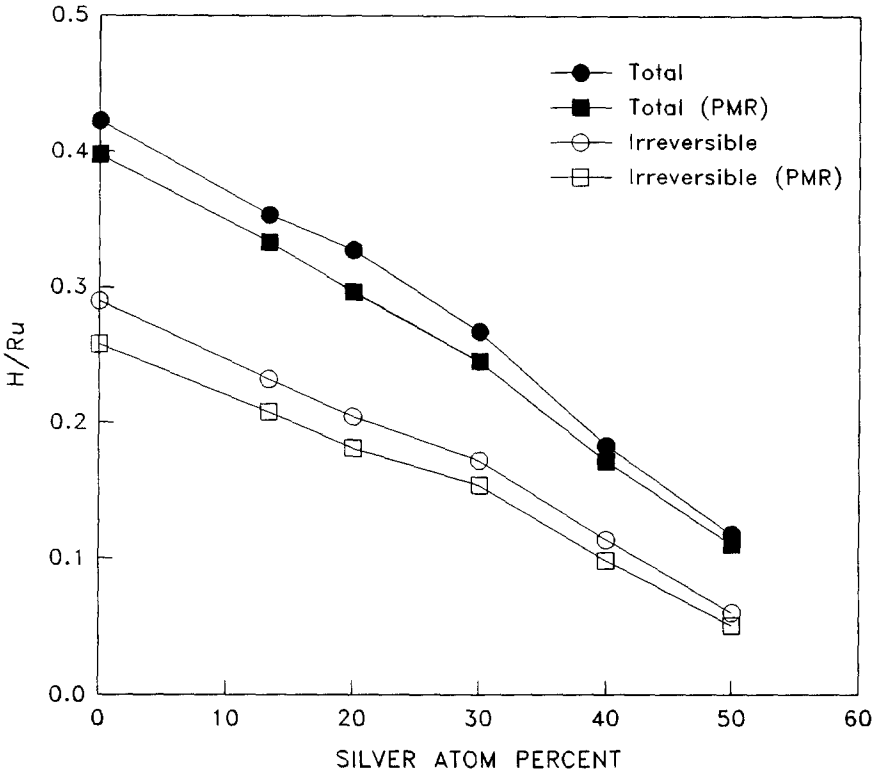

FIG. 4. The H/Ru ratios for both the total and the irreversible adsorption of hydrogen on a series of $Ru-Ag/SiO_2$ bimetallic catalysts. Results from measurements by both hydrogen chemisorption and ^1H NMR are shown for comparison.

the nitrate salt) and a 4% $Ru-Ag/SiO_2$ catalyst with 20 at.% silver content, respectively. These two spectra also show a small downfield shift of the upfield peaks in comparison with the corresponding spectra in Fig. 1. Obviously, the upfield peak intensity was suppressed to a greater extent by silver than by gold for the same Ag or Au atomic percentage.

While the upfield peak is asymmetric, the downfield peak corresponding to the silanol proton is symmetric in lineshape and can be fitted well with a Lorentzian line. By subtracting the downfield peak from the spectrum, the intensity of the upfield peak can be obtained by integrating the area under the peak. The intensity measurements for the upfield peak were performed on all the Ru/SiO_2, $Ru-Ag/SIO_2$, and $Ru-Au/SiO_2$ catalysts under various hydrogen pressures ranging from 5 to 30 Torr. As already observed on numerous pure Ru/SiO_2 catalysts (*20*), isotherms obtained in this manner also exhibit nearly straight lines over this hydrogen pressure range for $Ru-Ag/SiO_2$ and $Ru-Au/SiO_2$ bimetallic catalysts. The slopes of these isotherms match closely with those obtained by the volumetric method of hydrogen chemisorption. All isotherms were extrapolated to zero hydrogen pressure to obtain values of the H/Ru ratio.

The values of the H/Ru ratio for the total and the irreversible hydrogen adsorption on the $Ru-Ag/SiO_2$ catalysts as measured by both hydrogen chemisorption and NMR of adsorbed hydrogen are shown in Fig. 4 as functions of the silver content expressed in silver atomic percentage. Good agreement between the two techniques was found for both the total and the irreversible hydrogen

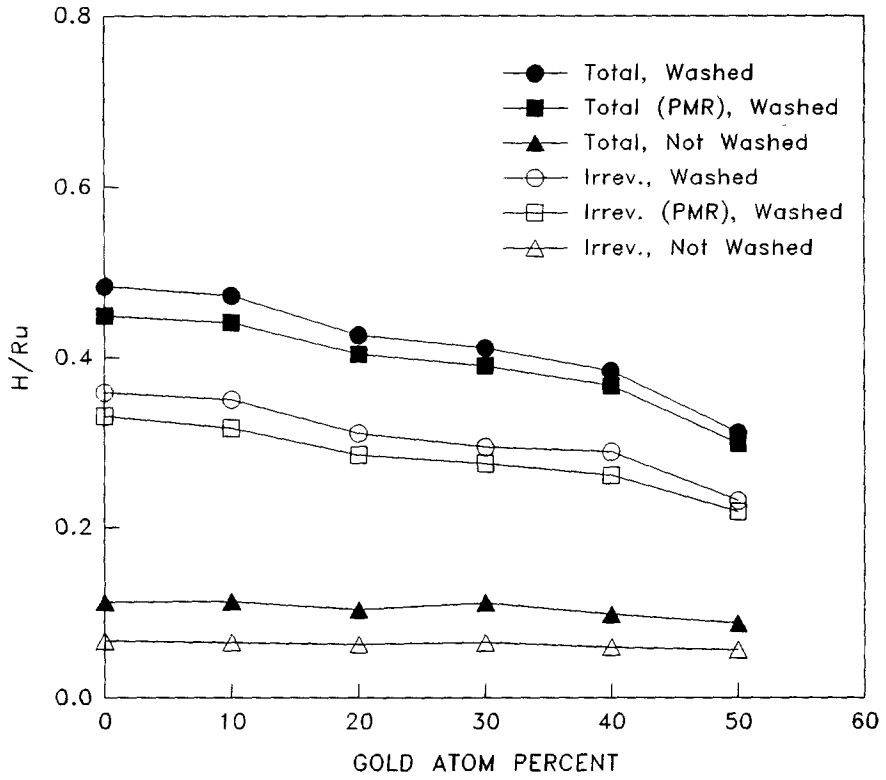

FIG. 5. The H/Ru ratios for both the total and the irreversible adsorption of hydrogen on a series of $Ru–Au/SiO_2$ bimetallic catalysts. Results from measurements by both volumetric technique and ^1H NMR on the washed catalysts (five washes) are shown for comparison. Also shown are the H/Ru ratios measured by the volumetric technique on the unwashed catalysts.

adsorption, although the NMR measurements consistently gave slightly lower H/Ru values. Suppression of the hydrogen chemisorption capacity of the pure Ru/SiO_2 catalyst by incorporation of silver was evident from the results in this figure as well as those in Fig. 1. This result is in agreement with that obtained by Rouco *et al.* (*2*).

Figure 5 shows the values of the H/Ru ratio for the total and the irreversible hydrogen adsorption as measured by both hydrogen chemisorption and NMR of adsorbed hydrogen on Ru/SiO_2 and $Ru–Au/SiO_2$ catalysts that were treated by hot water wash. Also shown are the results from hydrogen chemisorption on the unwashed Ru/SiO_2 and $Ru–Au/SiO_2$ catalysts. Again, good agreement between the two techniques on the washed Ru/SiO_2 and $Ru–Au/SiO_2$ catalysts was obtained for both the total and the irreversible hydrogen adsorption, with only small discrepancies.

Washing with hot water on the Ru/SiO_2 and $Ru–Au/SiO_2$ catalysts was carried out in steps. Hydrogen chemisorption and NMR measurements were taken on these catalysts after every wash. It was found that the hydrogen chemisorption capacity increased as the number of washes was increased and that this increase leveled off after five washes. This finding agrees with that reported by Miura *et al.* (*19*). It was concluded that after five washes chlorine was completely removed from the Ru/SiO_2 and $Ru–Au/SiO_2$ catalysts.

On the clean catalysts, addition of gold resulted in only a small decrease in the hydrogen chemisorption capacity, as shown

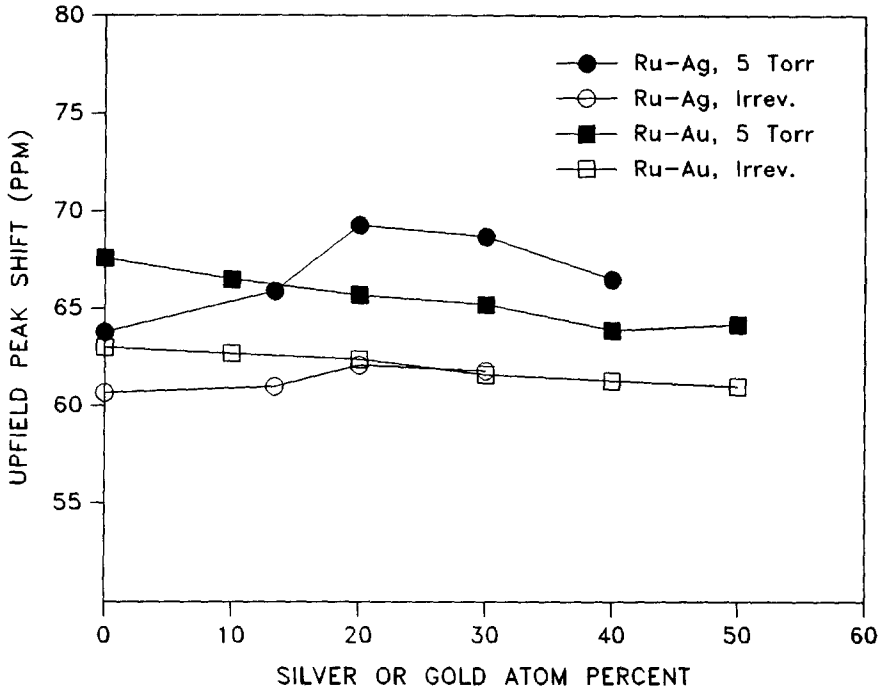

FIG. 6. Variations of the upfield lineshift with bulk metal compositions for both Ru–Ag/SiO_2 and Ru–Au/SiO_2 (five washes) bimetallic catalysts. Lineshift values for both 5 Torr hydrogen and the irreversible hydrogen are shown.

by the gradual decreasing trends of H/Ru ratio with increasing gold content in Fig. 5. The almost invariant trends of H/Ru ratio with increasing gold content for the chlorine-contaminated catalysts could be misleading because the effect of chlorine contamination rather than the effect of gold incorporation is dominating in this case. Clearly, chlorine suppresses the hydrogen chemisorption capacity by as much as 70 to 80% on Ru/SiO_2 and Ru–Au/SiO_2 catalysts. Shastri and Schwank (7) have reported a decrease in the hydrogen chemisorption capacity with increasing gold content on Ru–Au/SiO_2 catalysts, but in their study the ruthenium loading in the catalyst was not kept constant and chlorine-contaminated catalysts were used.

The lineshift values for the upfield peak on both the Ru–Ag/SiO_2 and the Ru–Au/SiO_2 (five washes) catalysts are shown in Fig. 6 under two conditions of hydrogen adsorption: (1) 5 Torr hydrogen, and (2) evacuated to 10^{-6} Torr for 10 min after adsorption under 5 Torr hydrogen. Lineshifts were observed for the Ru–Ag/SiO_2 catalysts farther upfield compared with those of the Ru/SiO_2 catalysts, especially for the ones with 20 at.% Ag and 30 at.% Ag in the case of the adsorption under 5 Torr hydrogen. Because of the diminishing intensity of the upfield peak at high silver contents (40 and 50 at.%), lineshift values in these cases become increasingly uncertain and are not reported here. On the other hand, sufficiently strong intensities of the upfield peaks for the Ru–Au/SiO_2 catalysts at high gold contents were present to determine the lineshift values. As shown in the figure, lineshifts remain essentially constant with only a small decrease with increasing gold content under both conditions of hydrogen adsorption. The discrepancy in lineshift values between the two Ru/SiO_2 catalysts

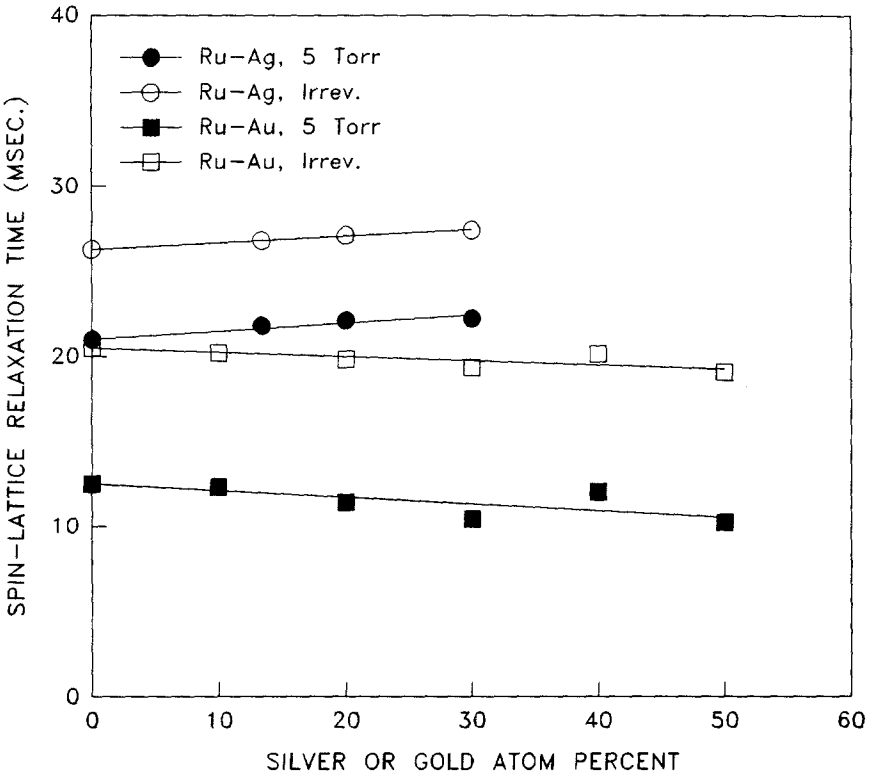

FIG. 7. Variations of spin-lattice relaxation times of hydrogen adsorbed on ruthenium with bulk metal compositions for both Ru–Ag/SiO_2 and Ru–Au/SiO_2 (five washes) bimetallic catalysts. Results for both 5 Torr hydrogen and the irreversible hydrogen are shown.

was due to variations in metal dispersion and particle sizes (*20*) resulting from different procedures in catalyst preparation.

The spin-lattice relaxation times for hydrogen adsorbed on ruthenium surfaces (upfield peak) in Ru/SiO_2, Ru–Ag/SiO_2, and Ru–Au/SiO_2 catalysts were measured by the inversion recovery technique in the frequency domain. The results are shown in Fig. 7 for both adsorption under 5 Torr hydrogen and evacuation to 10^{-6} Torr for 10 min after adsorption under 5 Torr hydrogen. As indicated in the figure, there exist a small increase of T_1 with increasing silver content and a small decrease of T_1 with increasing gold content. However, because the changes were comparable to the experimental uncertainty (±1 ms), the trends may be regarded as essentially constant over the range of Ag or Au content. Again, the discrepancy in T_1's between the two Ru/SiO_2 catalysts was due to variations in the ruthenium particle size.

Figure 8 shows the results of the spin-lattice relaxation times of the silanol proton on all Ru/SiO_2, Ru–Ag/SiO_2, and chlorine-free Ru–Au/SiO_2 catalysts under the two conditions of hydrogen adsorption mentioned above. The measurements were taken in the time domain by using inversion recovery. Since over 95% of the total proton population in the catalysts was in the form of the silanol group, any influence on the T_1 measurements from the hydrogen adsorbed on ruthenium was neglected. In all cases, there was an increase in T_1 as the silver or gold content was increased. However, a significant difference in the T_1

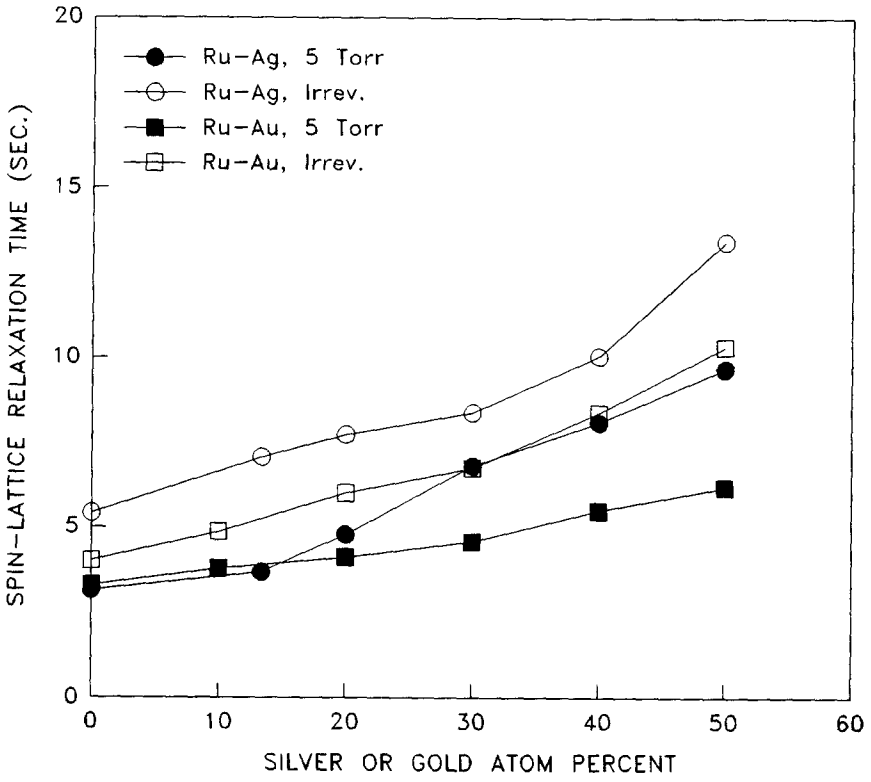

FIG. 8. Variations of spin-lattice relaxation times of the silanol proton with bulk metal compositions for both Ru–Ag/SiO_2 and Ru–Au/SiO_2 (five washes) bimetallic catalysts. Results for both 5 Torr hydrogen and the evacuation condition (10^{-6} Torr for 10 min after exposure to 5 Torr hydrogen) are shown.

trends between the silver and the gold series was observed, especially under the adsorption condition of 5 Torr hydrogen. A larger increase in T_1's of the silanol proton for Ru–Ag/SiO_2 catalysts is clearly shown in the figure in the case of 5 Torr hydrogen. Note that the spin-lattice relaxation times of the silanol proton on 4% Ru/SiO_2 and 4% Ru–Ag/SiO_2 catalysts were about 17 s as measured on samples without hydrogen dosage. The longest T_1's were observed for the Ru–Ag/SiO_2 series under the evacuation conditions after hydrogen dosage. As the silver content reached 50 at.%, a T_1 of about 14 s was measured under the evacuation condition, approaching the value measured under the condition of no hydrogen dosage.

DISCUSSION

Hydrogen Spillover

In a previous study on pure Ru/SiO_2 catalysts (*20*), the reversibly bound hydrogen on ruthenium surfaces has been determined to be the source of hydrogen spillover from the metal onto the silica support. In the same study, it has been proposed that the exchange of hydrogen atoms between the reversible hydrogen adsorbed on ruthenium and the silanol group occurs via the weakly adsorbed spiltover hydrogen, which acts as the intermediate for the exchange. A hydrogen–deuterium exchange experiment monitored by ^1H NMR clearly shows that the exchange process is much too slow at room temperature compared with T_1's of the si-

lanol group. For this reason, the observed shortening of T_1's of the silanol group upon introduction of hydrogen gas is attributed to spin-diffusion via a T_2 process among the spiltover hydrogen and the silanol proton rather than chemical exchange or spin-diffusion between the silanol protons. Thus, the value of the silanol proton T_1 is a monitor of the extent of hydrogen spillover (i.e., a higher degree of hydrogen spillover is indicated by a relatively shorter T_1 of the silanol proton). When this concept is applied to the Ru–Ag/SiO_2 and Ru–Au/SiO_2 systems, a suppression of hydrogen spillover from hydrogen adsorbed on ruthenium to the support is evident by the increase of silanol proton T_1 with increasing silver or gold content (Fig. 8). This suppressive effect on hydrogen spillover is stronger for silver than for gold. The observation is consistent with the fact that silver suppresses the amount of the reversibly adsorbed hydrogen on ruthenium to a greater extent than does gold (Figs. 4 and 5).

On the Ru–Ag/SiO_2 and Ru–Au/SiO_2 catalysts investigated in the present study, there is no indication from the NMR measurements of any resonance arising from hydrogen adsorbed on silver or gold. Only resonances associated with the silanol proton and hydrogen adsorbed on ruthenium are observed. Therefore, the amount of hydrogen adsorbed on Ru in these bimetallic catalysts can be measured directly by NMR without any complication of hydrogen spillover from ruthenium to silver or gold, unlike the case of Ru–Cu bimetallic system (*14, 15*).

For these two bimetallic systems, hydrogen spillover from ruthenium to the silica support presents the only intrinsic error in measuring the amount of hydrogen adsorbed on ruthenium exposed at surface by the volumetric technique. In the case of total hydrogen adsorption, where reversibly adsorbed hydrogen is present on ruthenium, the small discrepancy in the H/Ru ratio observed by the volumetric technique and that determined by NMR may be due to this hydrogen spillover effect. However, since the amount of spiltover hydrogen is less than 10% of the total hydrogen adsorption at room temperature, experimental errors in spin counting, volumetric measurements, or both may contribute to the discrepancy as well.

Hydrogen Adsorbed on Ru–Ag and Ru–Au Bimetallics

Since there is no hydrogen spillover from ruthenium to silver or gold, one may expect to observe the same spectral features in the proton NMR on Ru–Ag/SiO_2 or Ru–Au/SiO_2 catalysts as those observed with the Ru/SiO_2 catalysts. This result is found for the Ru–Au/SiO_2 catalysts (washed), which show essentially no changes in NMR linewidth, lineshift, and the spin-lattice relaxation time of the hydrogen adsorbed on ruthenium with increasing gold content. This means that incorporation of gold has little or no influence on the local electronic environment of the surface ruthenium atoms. However, different NMR spectral features have been observed on the Ru–Ag/SiO_2 catalysts, most noticeably the lineshape and lineshift of the upfield peak corresponding to hydrogen adsorbed on ruthenium. The asymmetric lineshape of the upfield peak on Ru/SiO_2 under 5 Torr hydrogen (Fig. 1) may be due to many factors such as orientational chemical shift anisotropy, varied shifts on different adsorption sites, or varied distribution of the irreversible and the reversible hydrogen on these adsorption sites. Since the same Ru loading was used, the metal particle size is expected to remain roughly constant between Ru/SiO_2 and Ru–Ag/SiO_2 catalysts. Thus the chemical shift anisotropy and the effect of magnetic susceptibility are not expected to change significantly between these catalysts and are not inferred to be the cause of the changes in lineshape and lineshift (Figs. 1 and 6).

For the Ru–Ag/SiO_2 series the dispersion of pure Ru/SiO_2 catalysts as measured by the amount of irreversibly adsorbed hydro-

gen was 0.29. At this dispersion, a substantial fraction (about 20%) of the ruthenium atoms exposed at the surface are located at the defect-like edge and corner positions of the metal particles. If the hydrogen adsorbed on these sites exhibits a shift that is somewhat farther downfield relative to that adsorbed on basal plane Ru atoms, then the asymmetric lineshape for the pure Ru/SiO_2 catalyst may be accounted for. As silver atoms are introduced into the system, they deposit preferentially at the low coordination sites before covering the basal planes of Ru particles, as is the case with most strongly surface-segregating systems (*24*). As a consequence, the resonance line becomes symmetrical and the apparent (overall) lineshift moves farther upfield with increasing content of Ag. Conceivably, a similar effect could occur on $Ru–Au/SiO_2$ catalysts. However, since gold has the tendency to form three-dimensional particles rather than to spread out on surfaces of Ru particles (see discussion below), its influence on the NMR spectral features is far less pronounced than that of silver.

Suppression of hydrogen chemisorption capacity by chlorine contamination on Ru/SiO_2 and $Ru–Au/SiO_2$ catalysts is striking (Figs. 2 and 5). The effect of chlorine is more than just preferential blocking of certain sites, as noted for silver. With chlorine present, a downfield shift of the upfield peak was observed (Fig. 2). The magnitude of the shift indicates a change in the local electronic environment of the adsorption sites associated with the chlorine contamination at surfaces of Ru and Ru–Au particles. This electronic interaction may be a direct chemical shift or an indirect one via the metal Knight shift. The latter explanation would seem to be more reasonable since the observed shift was larger than the usual values for chemical shift. Bonding between chlorine and surface Ru atoms may result in increased localization of the Ru 4*d* valence electrons and less spin polarization influencing the adsorbed hydrogen atoms.

Comparison among Ru–Group IB Bimetallics

Figure 9 presents variations of the relative fractional Ru dispersion as functions of Cu, Ag, and Au content expressed in metal atomic percentages. For the $Ru–Ag/SiO_2$ and $Ru–Au/SiO_2$ (washed) catalysts, the Ru dispersion was obtained from the H/Ru ratio of the irreversibly adsorbed hydrogen measured by NMR. All values of the fractional Ru dispersion for $Ru–Ag/SiO_2$ and $Ru–Au/SiO_2$ catalysts were normalized to the respective Ru dispersion of the pure Ru/SiO_2 catalyst in the series (0.29 and 0.36, respectively). The values of the normalized fractional Ru dispersion for the $Ru–Cu/SiO_2$ series were obtained from the surface composition determined by NMR in a previous study (*15*). The surface composition was converted to the fractional Ru dispersion by multiplying it by the corresponding H/Ru value as measured by chemisorption of the irreversibly adsorbed hydrogen. Thus, a direct comparison can be made on a common basis among these three classes of bimetallic catalysts. Also shown in Fig. 9 is a set of calculated values of the normalized fractional Ru dispersion by assuming a one-to-one monolayer growth of the second metallic element (Cu, Ag, or Au) on Ru surfaces.

The above results show that different trends in fractional Ru dispersion are present for these three ruthenium-containing bimetallic catalysts. The results are taken to indicate the differences in interaction at the interface between ruthenium and copper, silver, or gold. Copper covers the ruthenium surfaces in a monolayer fashion until a high copper coverage (78%) is reached. Then, growth of three-dimensional copper islands on ruthenium surfaces begins as more copper is added to the system (*15*). Silver interacts with the ruthenium surfaces to a lesser extent, covering the same fraction of the ruthenium surfaces at much higher bulk composition (atomic percentage) than copper. Gold has little in-

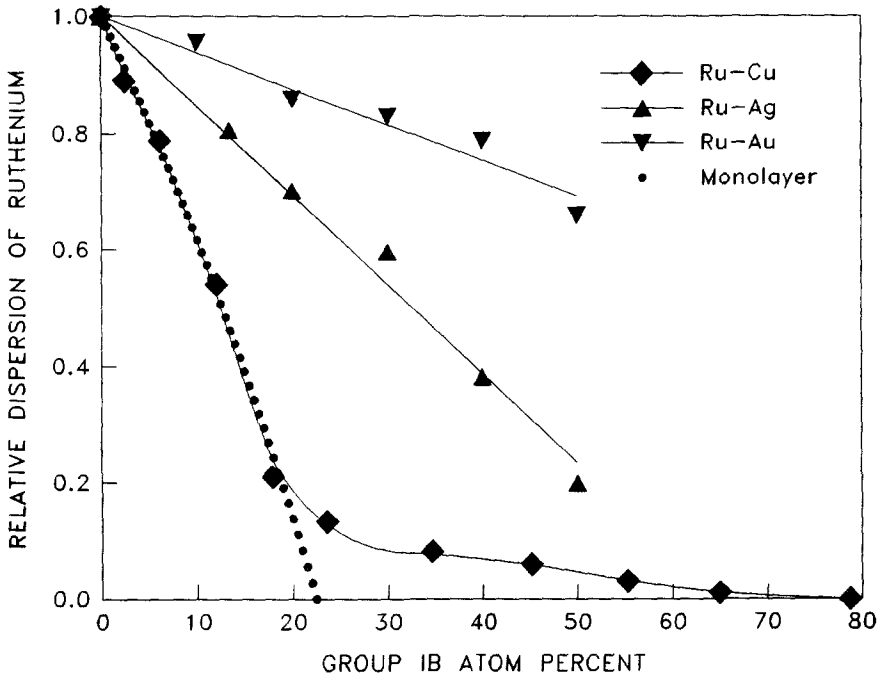

FIG. 9. Plot of relative fractional Ru dispersion as functions of the copper, silver, and gold contents for a series of Ru–Cu/SiO_2, Ru–Ag/SiO_2, and Ru–Au/SiO_2 (washed) bimetallic catalysts, respectively. The fractional Ru dispersion for the bimetallics is normalized to the dispersion for the respective pure Ru/SiO_2 catalyst in the series. The normalized fractional Ru dispersion corresponding to a monolayer growth of a second metal on Ru is also shown for comparison.

teraction with ruthenium surfaces and tends to form three-dimensional islands on the Ru surfaces or separate gold particles in the support.

The fractional dispersion results for the ruthenium copper catalysts shown in Fig. 9 are in good agreement with Monte Carlo simulations (*11*) which indicate that copper will segregate almost completely to the surface. At low copper concentrations the defect-like edge and corner sites exhibit the strongest driving force for segregation. Experimental evidence for the preferential population of ruthenium defect site by copper has been presented by Kim *et al.* (*25*). Once nearly all the edge and corner lattice positions are populated by copper, the basal planes are covered by pseudomorphic two-dimensional islands of copper. This monolayer growth of copper overlayers on ruthenium surfaces has been noted in various studies employing ruthenium single crystals (*25–28*). In addition, results from studies of small Ru–Cu bimetallic particles indicate that a core of ruthenium is surrounded by a thin layer of copper (*25–33*).

The results given in Fig. 9 indicate that neither the Ru–Ag nor the Ru–Au system displays such strong interaction between the constituent metals as does Ru–Cu. This behavior may be understood by noting the values of the bulk cohesive energy (as indicated by the heat of sublimation) for the group Ib metals compared to those of ruthenium and by noting the estimated heats of mixing for the three bimetallic systems (see Table 1). All three bimetallic systems have an estimated heat of mixing that is large and endothermic. For this reason bulk alloys are not formed. The differences in the cohesive energies, however, indicate that forming a ruthenium surface relative to any of

TABLE 1

	ΔH_{sub}[a] (298) (kJ/mol)
Ru	651.8
Ag	284.2
Au	368.4
Cu	337.0
	ΔH_{mix}[b] (kJ/mol)
Ru–Ag	34
Ru–Au	23
Ru–Cu	17

[a] Data from Ref. (*34*).
[b] Estimate from Ref. (*35*).

the group Ib metals is energetically unfavorable. A comparison of the values given in Table 1 shows that covering ruthenium particles with copper results in a considerable lowering of the energy of the system. Less energy is saved when silver covers ruthenium. Because of the higher cohesive energy of gold relative to that of copper, the tendency for gold to form a thin layer on ruthenium is significantly less than that for copper. As shown in Fig. 9, gold and ruthenium display little tendency to form true bimetallic systems. This view is consistent with the microdiffraction study of Cowley and Plano (*9*), who observed no direct association of gold and ruthenium for particles in the range 1 to 3 nm.

CONCLUSIONS

NMR of adsorbed hydrogen indicates no spillover of hydrogen from ruthenium to either silver or gold in Ru–Ag/SiO_2 and Ru–Au/SIO_2 catalysts. Hydrogen spillover from the reversibly adsorbed hydrogen on Ru onto the silica support is suppressed by addition of silver or gold. This effect is more pronounced in Ru–Ag/SiO_2 catalysts, as indicated by the much longer spin-lattice relaxation times of the silanol proton in the support. The preferential location of silver atoms on defect-like ruthenium sites assists in the differentiation of hydrogen adsorbed on the various ruthenium sites. Gold does not form bimetallics with ruthenium as efficiently as silver. This is indicated by the smaller variation in hydrogen chemisorption capacity measured by both the NMR and the volumetric technique. Both techniques clearly show the poisoning effect of residual chlorine on the hydrogen chemisorption capacity of the Ru/SiO_2 catalyst and Ru–Au/SiO_2 bimetallic catalysts. A direct comparison between clean Ru–Cu/SiO_2, Ru–Ag/SiO_2, and Ru–Au/SiO_2 bimetallic catalysts indicates that copper has the strongest tendency to cover surfaces of ruthenium particles among Group IB metals.

ACKNOWLEDGMENTS

This work was supported by the U.S. Department of Energy, Office of Basic Energy Science, Contract W-7405-ENG-82. The support of the Engineering Research Institute of Iowa State University is also acknowledged.

REFERENCES

1. Sinfelt, J. H., Barnett, A. E., and Carter, J. L., U.S. Patent 3,617,518, Nov. 2, 1971.
2. Rouco, A. J., Haller, G. L., Oliver, J. A., and Kemball, C., *J. Catal.* **84,** 297 (1983).
3. Damiani, D. E., Perez Millan, E. D., and Rouco, A. J., *React. Kinet. Catal. Lett.* **36,** 15 (1988).
4. Bassi, I. W., Garbassi, F., and Vlaic, G., *J. Catal.* **64,** 405 (1980).
5. Galvagno, S., Schwank, J., and Parravano, G., *J. Catal.* **69,** 283 (1981).
6. Datye, A. K., and Schwank, J., *J. Catal.* **93,** 256 (1985).
7. Shastri, A. G., and Schwank, J., *J. Catal.* **95,** 271 (1985).
8. Shastri, A. G., and Schwank, J., *J. Catal.* **95,** 284 (1985).
9. Cowley, J. M., and Plano, R. J., *J. Catal.* **108,** 199 (1987).
10. Hansen, M., "Constitution of Binary Alloys," 2nd ed., p. 45 and p. 230. McGraw-Hill, New York, 1958.
11. Smale, M. W., and King, T. S., *J. Catal.* **119,** 441 (1989).
12. Wu, X., Smale, M. W., Gerstein, B. C., and King, T. S., Paper No. 15a, AIChE Annual Meeting, New York, November 1987.
13. Hayward, D. O., and Trapnell, B. M., "Chemisorption," 2nd ed., p. 75 and p. 233. Butterworths, Washington, 1964.
14. King, T. S., Wu, X., and Gerstein, B. C., *J. Amer. Chem. Soc.* **108,** 6056 (1986).
15. Wu, X., Gerstein, B. C., and King, T. S., *J. Catal.* **121,** 271 (1990).

16. Marita, T., Miura, H., Sugiyama, K., Matsuda, T., and Gonzalez, R. D., *J. Catal.* **103,** 492 (1987).
17. Lu, K., and Tatarchuk, B. J., *J. Catal.* **106,** 166 (1987).
18. Lu, K., and Tatarchuk, B. J., *J. Catal.* **106,** 176 (1987).
19. Miura, H., Hondou, H., Sygiyama, K., Matsuda, T., and Gonzalez, R. D., *in* "Proceedings, 9th International Congress on Catalysis" (M. J. Phillips and M. Terman, Eds.), p. 1307. Chem. Institute of Canada, Ottawa, 1988.
20. Wu, X., Gerstein, B. C., and King, T. S., *J. Catal.* **118,** 238 (1989).
21. Cheung, T. T. P., Worthington, L. E., Murphy, P. D. B., and Gerstein, B. C., *J. Magn. Reson.* **41,** 158 (1980).
22. Fry, C. G., Iwamiya, J. H., Apple, T. M., and Gerstein, B. C., *J. Magn. Res.* **63,** 214 (1985).
23. Gerstein, B. C., "Alternating Circuit Theory and Pulsed NMR," IS-49244C-13, Available from NTIS, U.S. Dept. of Commerce, 5265 Port Royal Road, Springfield, VA 22161.
24. Strohl, J. K., and King, T. S., *J. Catal.* **116,** 540 (1989).
25. Kim, K. S., Sinfelt, J. H., Eder, S., Markert, K., and Wandelt, K., *J. Phys. Chem.* **91,** 2337 (1987).
26. Goodman, D. W., and Peden, C. H. F., *J. Catal.* **95,** 321 (1985).
27. Yates, J. T., Peden, C. H., and Goodman, D. W., *J. Catal.* **94,** 576 (1985).
28. Peden, C. H. F., and Goodman, D. W., *Ind. Eng. Chem. Fundam.* **25,** 58 (1986).
29. Houston, J. E., Peden, C. H. F., Feibelman, P. J., and Hamann, D. R., *Phys. Rev. Lett.* **56,** 375 (1986).
30. Sinfelt, J. H., *Acc. Chem. Res.* **10,** 15 (1977).
31. Sinfelt, J. H., Lam, Y. L., Cusumano, J. A., and Barnett, A. E., *J. Catal.* **42,** 227 (1976).
32. Sinfelt, J. H., *Science* **195,** 641 (1977).
33. Sinfelt, J. H., Via, G. H., and Lytle, F. W., *J. Chem. Phys.* **72,** 4832 (1980).
34. Hultgren, R., Desai, P. D., Hawkins, D. T., Gleiser, M., Kelley, K. K., and Wagman, D. D., "Selected Values of the Thermodynamic Properties of the Elements," American Society for Metals, Metals Park, OH 1973.
35. Miedema, A. R., *Philips Tech. Rev.* **36**(8), 217 (1976).